Synergy of Nanocrystalline Carbon Nitride with Cu Single Atom Catalyst Leads to Selective Photocatalytic Reduction of CO_2 to Methanol

Tara M. LeMercier,[a] Madasamy Thangamuthu,*[a] Emerson C. Kohlrausch,[a] Yifan Chen,[a] Craig T. Stoppiello,[b] Michael W. Fay,[b] Graham A. Rance,[b] Gazi N. Aliev,[c] Wolfgang Theis,[c] Johannes Biskupek,[d] Ute Kaiser,[d] Anabel E. Lanterna,[a] Jesum Alves Fernandes,[a] and Andrei N. Khlobystov*[a]

[a]School of Chemistry, University of Nottingham, University Park, Nottingham NG7 2RD, United Kingdom

[b]Nanoscale and Microscale Research Centre (nmRC), University of Nottingham, Nottingham, NG7 2QL, United Kingdom

[c]School of Physics and Astronomy, University of Birmingham, Edgbaston, Birmingham B15 2TT, United Kingdom

[d]Electron Microscopy Group of Materials Science, Ulm University, 89081 Ulm, Germany

E-mail: andrei.khlobystov@nottignham.ac.uk, madasamy.thangamuthu1@nottingham.ac.uk

Supporting information

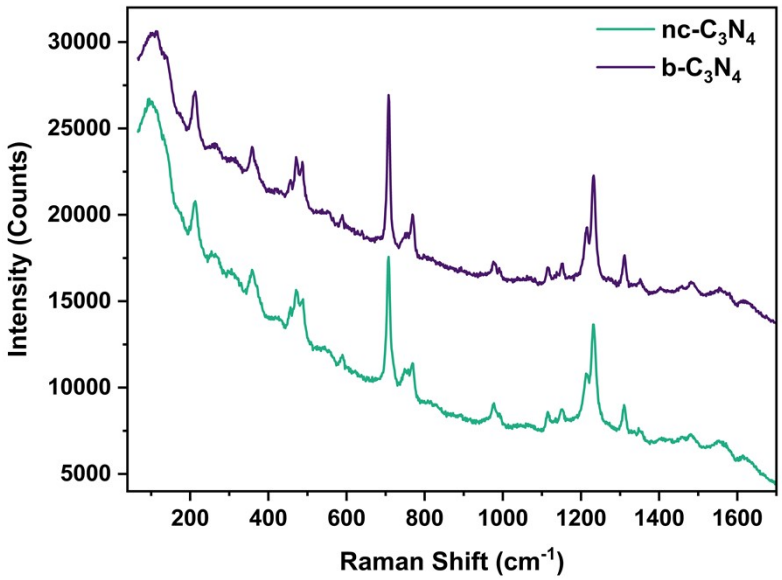

Figure S1. Raman analysis with a 785 nm laser indicates melon structure for both materials and b-C_3N_4 baseline fluorescence is higher due to a higher rate of charge recombination.

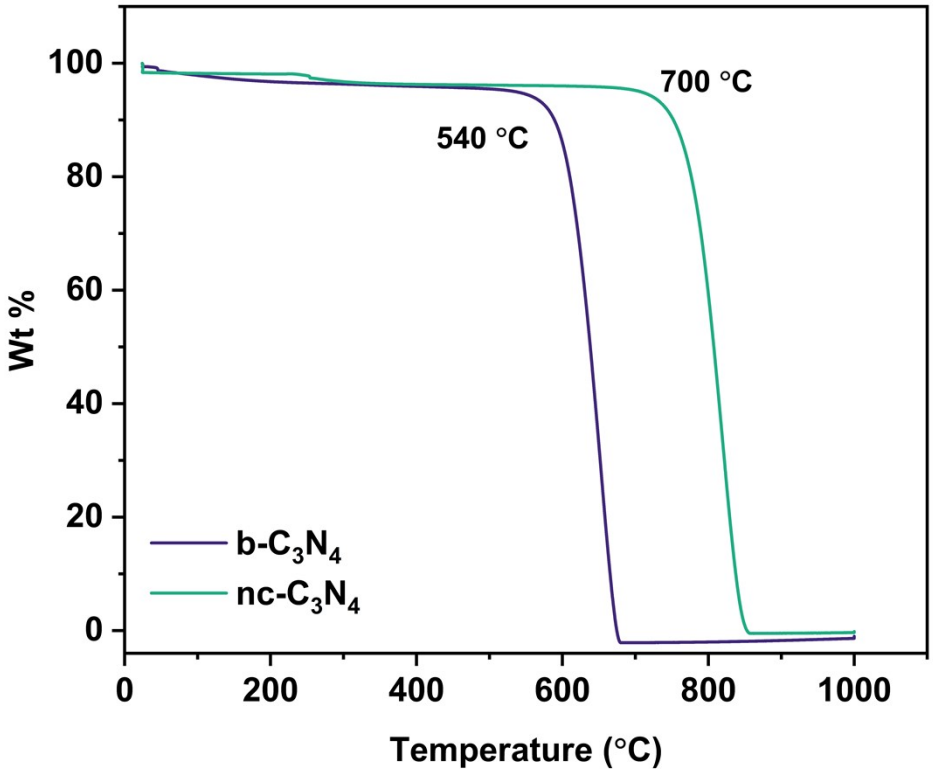

Figure S2. TGA in air shows oxidation onset temperature increases for nc-C_3N_4 (from 540 °C to 700 °C).

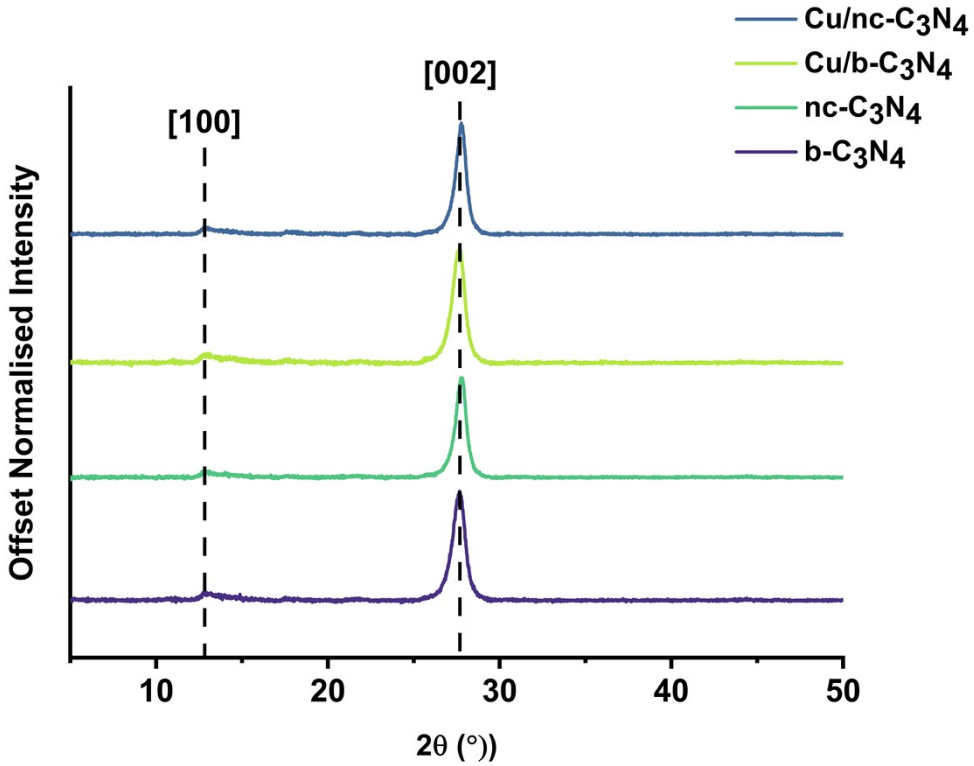

Figure S3. Powder XRD comparison of all materials: Cu/nc-C_3N_4 (dark blue) and Cu/b-C_3N_4 (light green) show no diffractions related to Cu and only have those pertinent to C_3N_4 materials. nc-C_3N_4 (dark green) and b-C_3N_4 (purple) show diffractions (100) related to the in-plane tri-s-triazine and (002) related to the interlayer stacking.

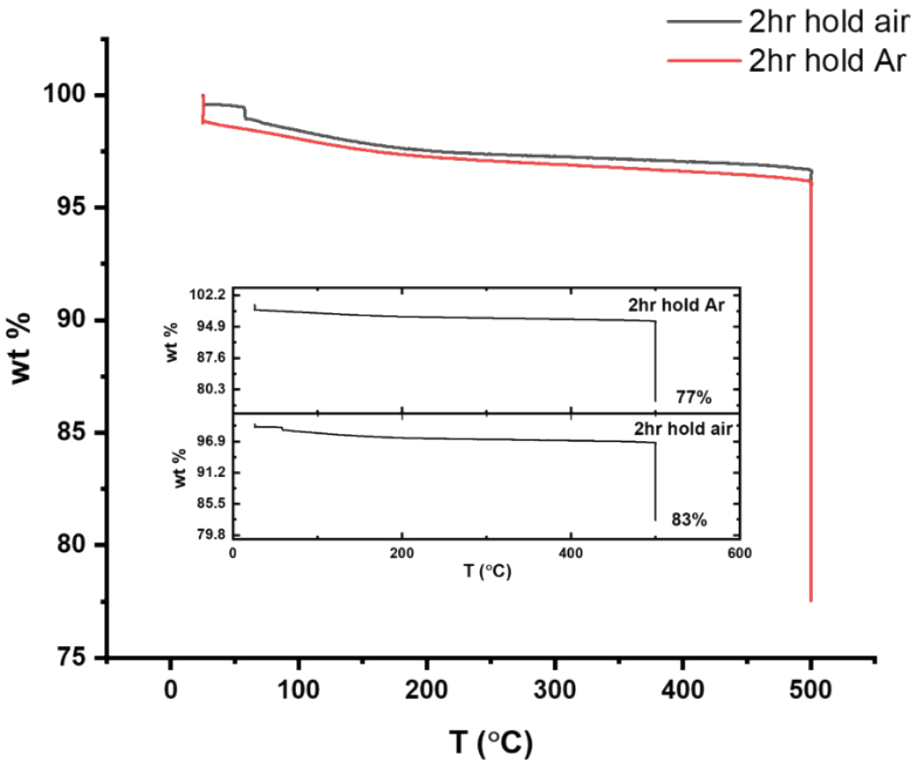

Figure S4. TGA of nc-C_3N_4 emulating reaction conditions (500 °C, 2hr) in air (black) and Ar (Red). It is observed (insert) that thermal treatment in air shows higher residual weight. Suggesting that some oxidation has occurred.

Table S1: N 1s XPS results for C_3N_4 materials, including % peak area.

Sample	State	Binding Energy (eV)	Peak Area	% Peak Area
b-C_3N_4	*C-N=C*	*398.6*	*7926.71*	*45.2*
	N-$(C)_3$	*399.7*	*4743.46*	*27.0*
	C-N-H	*401.0*	*4877.56*	*27.8*
nc-C_3N_4	*C-N=C*	*398.6*	*14900.75*	*65.3*
	N-$(C)_3$	*399.8*	*5169.3*	*22.7*
	C-N-H	*401.4*	*2753.38*	*12.0*

Table S2: Cu $p_{3/2}$ XPS results for C_3N_4 materials, including % peak area.

Sample	Oxidation State	Binding Energy (eV)	Peak Area	% Peak Area
b-C_3N_4	*Cu^I*	*932.66*	*2894.94*	*44.1*
	Cu^{II}	*934.18*	*2406.05*	*36.7*
	Cu^{II} Sat2	*939.00*	*774.71*	*11.8*
	Cu^I Sat1	*943.84*	*484.38*	*7.4*
nc-C_3N_4	*Cu^I*	*932.48*	*3088.2*	*63.7*
	Cu^{II}	*934.67*	*1220.03*	*25.2*
	Cu^{II} Sat2	*941.6*	*412.27*	*2.6*
	Cu^I Sat1	*944.29*	*127.75*	*8.5*

Table S3: C 1s XPS results for C_3N_4 materials, including % peak area.

Sample	Oxidation State	Binding Energy (eV)	Peak Area	% Peak Area
b-C_3N_4	*C-C*	*284.8*	*2171.28*	*17.8*
	C-OH	*286.2*	*1240.01*	*10.2*
	C-$(N)_3$	*288.3*	*6557.01*	*53.7*
	C-NH	*290.2*	*2250.07*	*18.4*
nc-C_3N_4	*C-C*	*284.8*	*2171.28*	*22.7*
	C-OH	*286.2*	*971.99*	*6.6*
	C-$(N)_3$	*288.1*	*8621.38*	*58.3*
	C-NH	*289.3*	*1840.47*	*12.5*

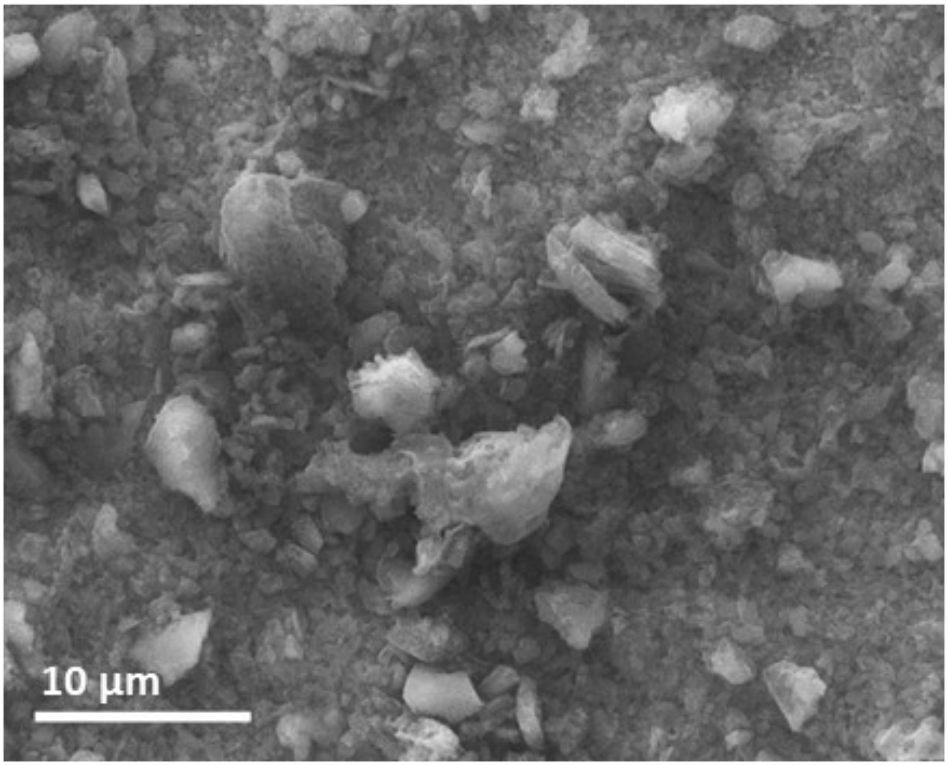

Figure S5. SEM image of b-C_3N_4 particles. Note the non-uniform morphology and broad size distribution (1-10 µm).

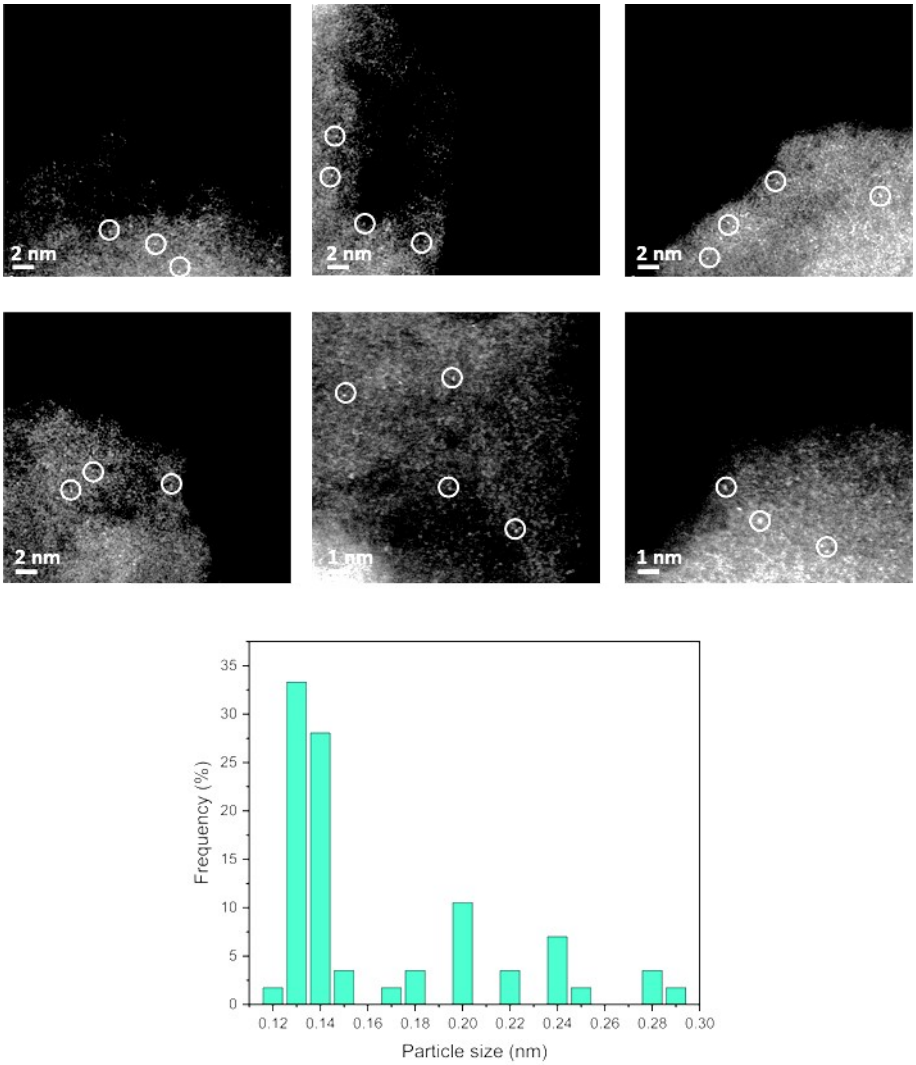

Figure S6. AC-STEM images from which particle analysis reveals single atoms (white circles) have a prevalence of around 70 % with the remainder of clusters not exceeding 3 atoms.

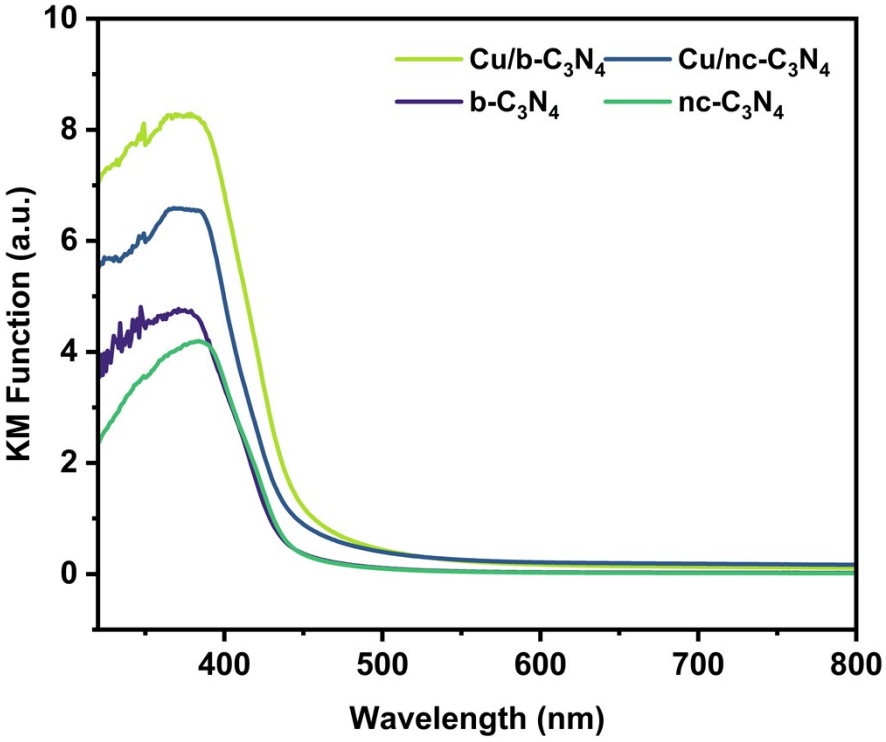

Figure S7. UV-Vis absorption spectra are shown for all materials to have an edge commencing at 450 nm, with a peak at 375 nm (black dotted line). Cu-containing materials show higher absorption intensities.

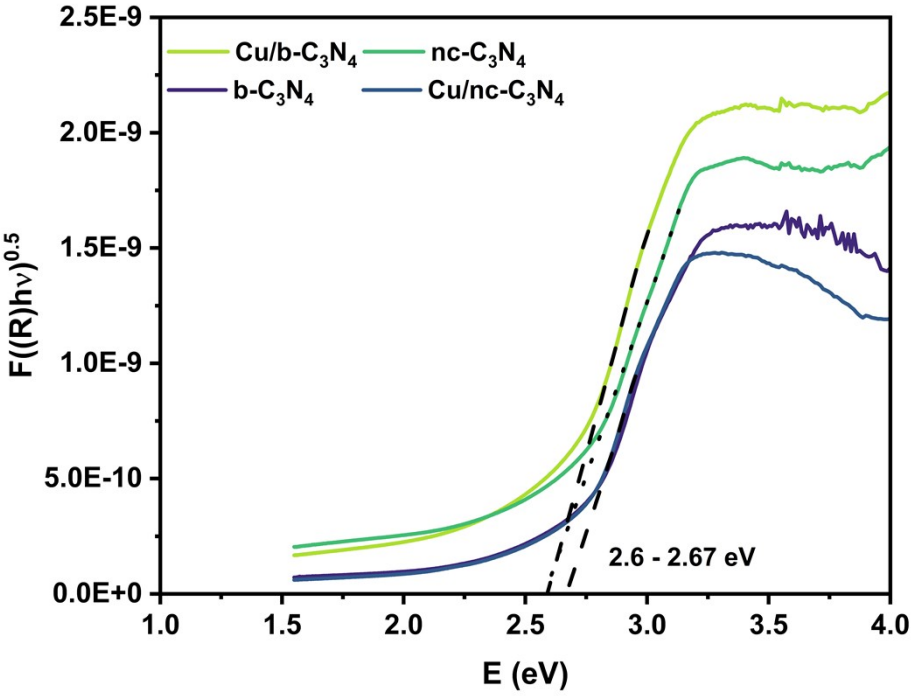

Figure S8. Tauc Plot analysis shows materials have a bang gap between 2.6 and 2.67 eV (dot/dash intercept extrapolation).

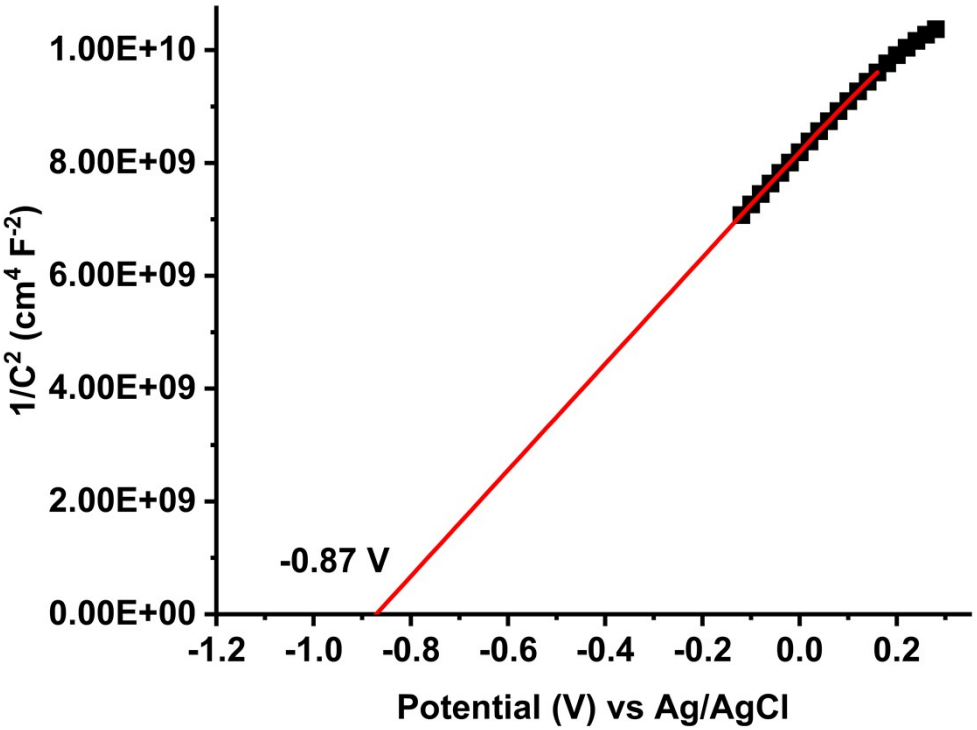

Figure S9. Linear region of flat band potential of b-C_3N_4 (black dots). Intercept extrapolation (red line) shows a conduction band potential of -0.87 V vs Ag/AgCl.

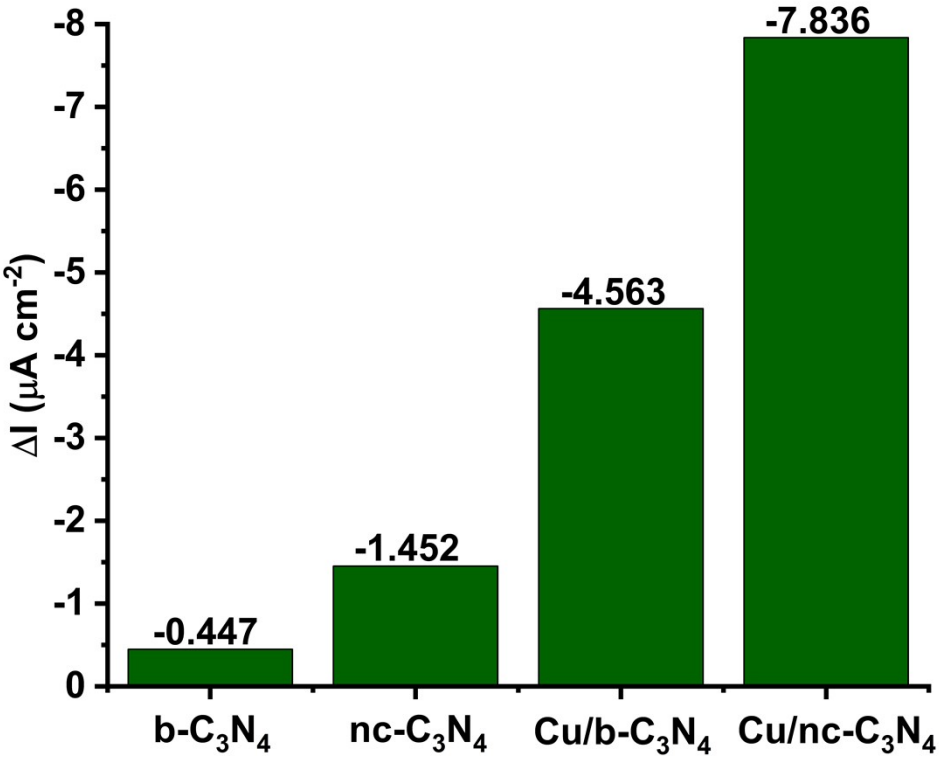

Figure S10. Change in current density observed from photocurrent response measurements.

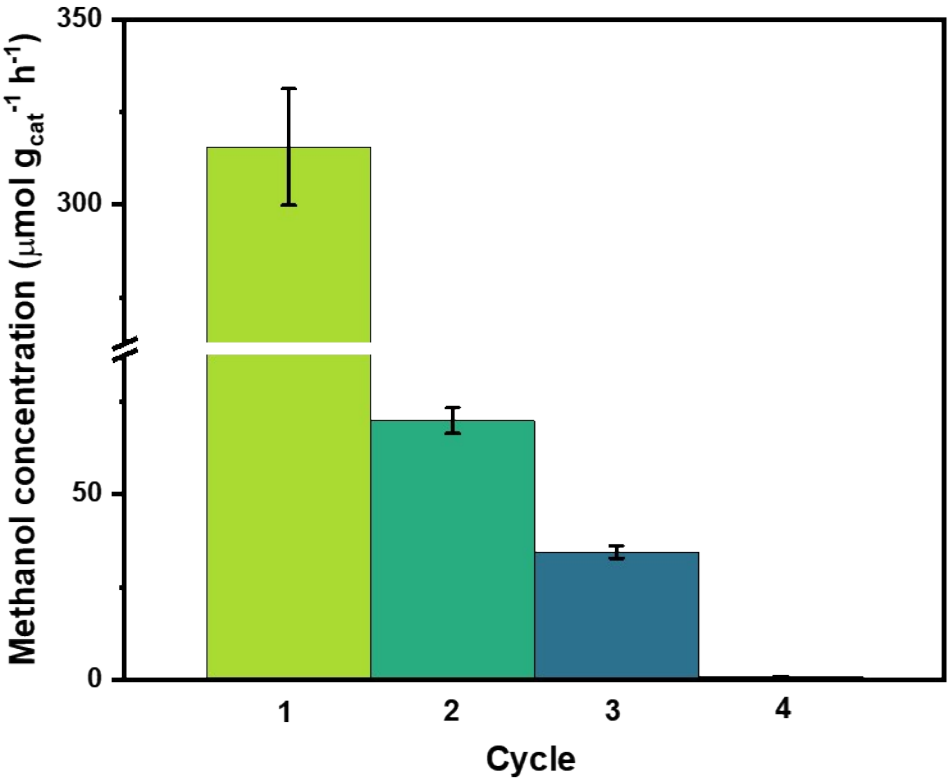

Figure S11. The stability of Cu/nc-C_3N_4 for prolonged methanol production was tested by measuring the methanol concentration for 8 h (composed of 4 consecutives 2 h runs). A 77% decrease in activity is observed during the second cycle (70 μmol g_{cat}^{-1} h^{-1}) and further by 50% during the third cycle (34 μmol g_{cat}^{-1} h^{-1}). Methanol is only found in trace amounts upon the fourth cycle. These results suggest that the present Cu/nc-C_3N_4 catalyst might have changed over time, or the methanol produced during the reaction may be consumed as a hole-scavenger by a long-term reaction. It strongly suggests that product separation is crucial as soon as it is produced during the reaction.

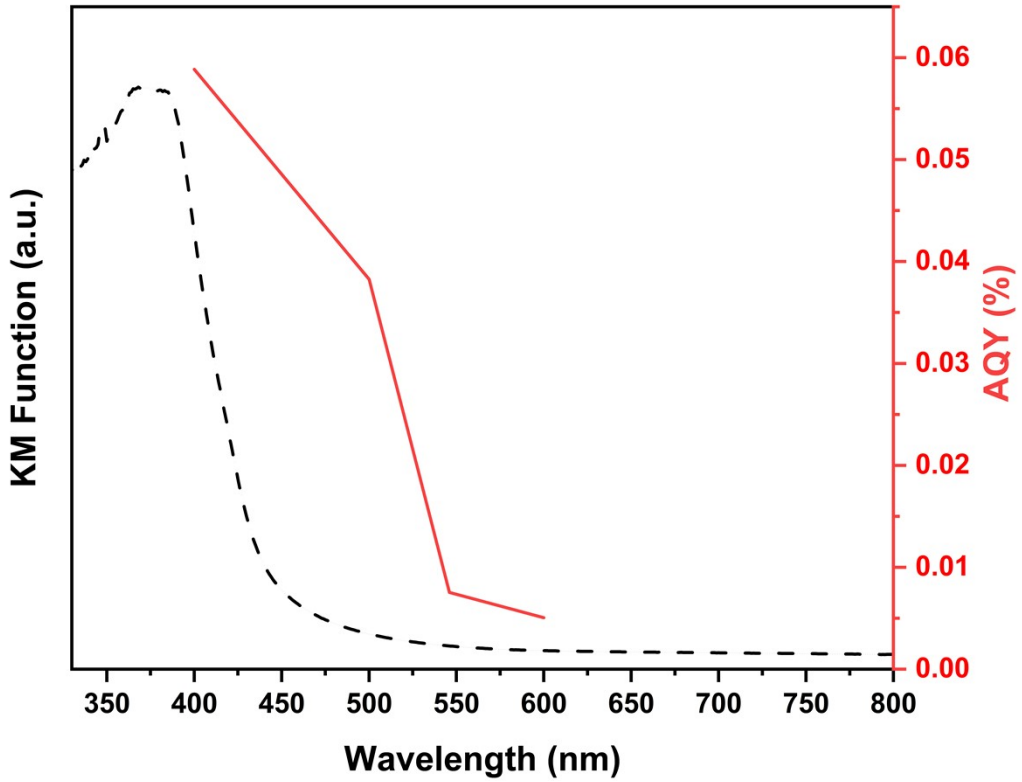

Figure S12. The AQY was obtained using Cu/nc-C_3N_4 (red line) for CH_4 and CH_3OH and the absorption profile of Cu/nc-C_3N_4 (black dotted line).

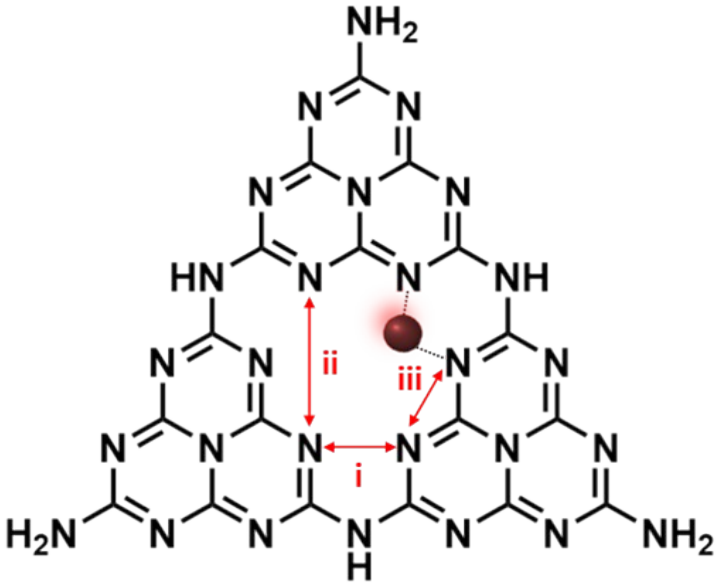

Figure S13. Tri-s-triazine vacancy of C_3N_4 with spacing corresponding to i) 0.26 nm; ii) 0.42 nm and iii) 0.23 nm. Cu(I) with radius 0.074 nm (red circle) is most likely to bind at sites i) assuming theoretical Cu-N bond length values of 0.196 nm.[1]

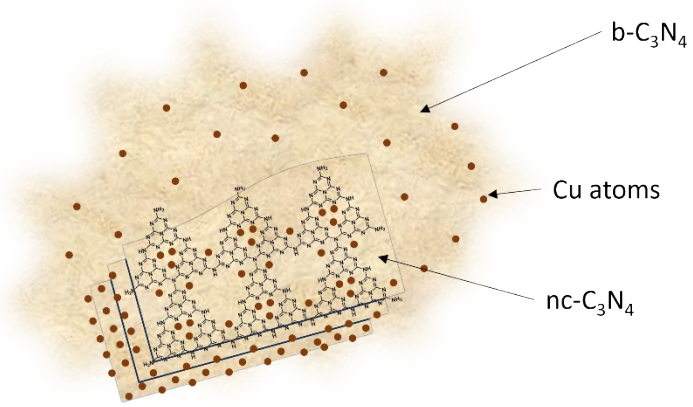

Figure S14. Schematic representation of the Cu binding to nc-C_3N_4 sites achieved through the increased crystallinity, and dangling bonds in these regions.

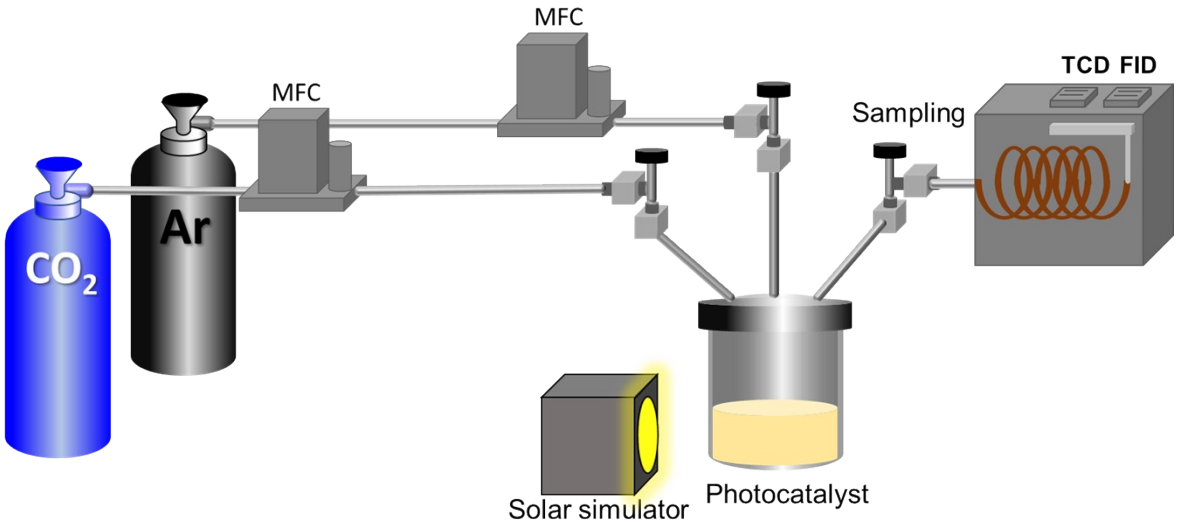

Figure S15. Schematic of custom-built Pyrex continuous flow photoreactor equipped with two mass flow controllers. Reactor volume: 28.5 mL, total pipeline volume 5.3 mL.

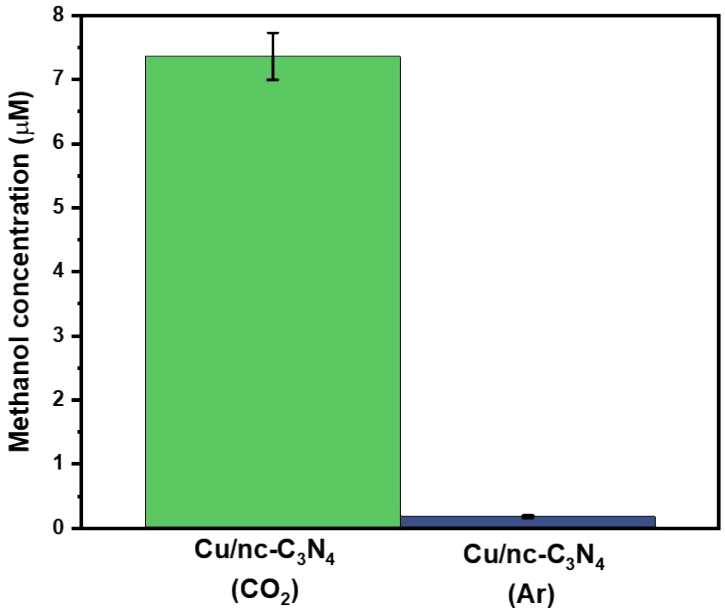

Figure S16. Control reaction under Ar (blue) conditions show trace amounts of methanol observed by NMR spectroscopy when compared to the catalyst under CO_2 saturation (green).

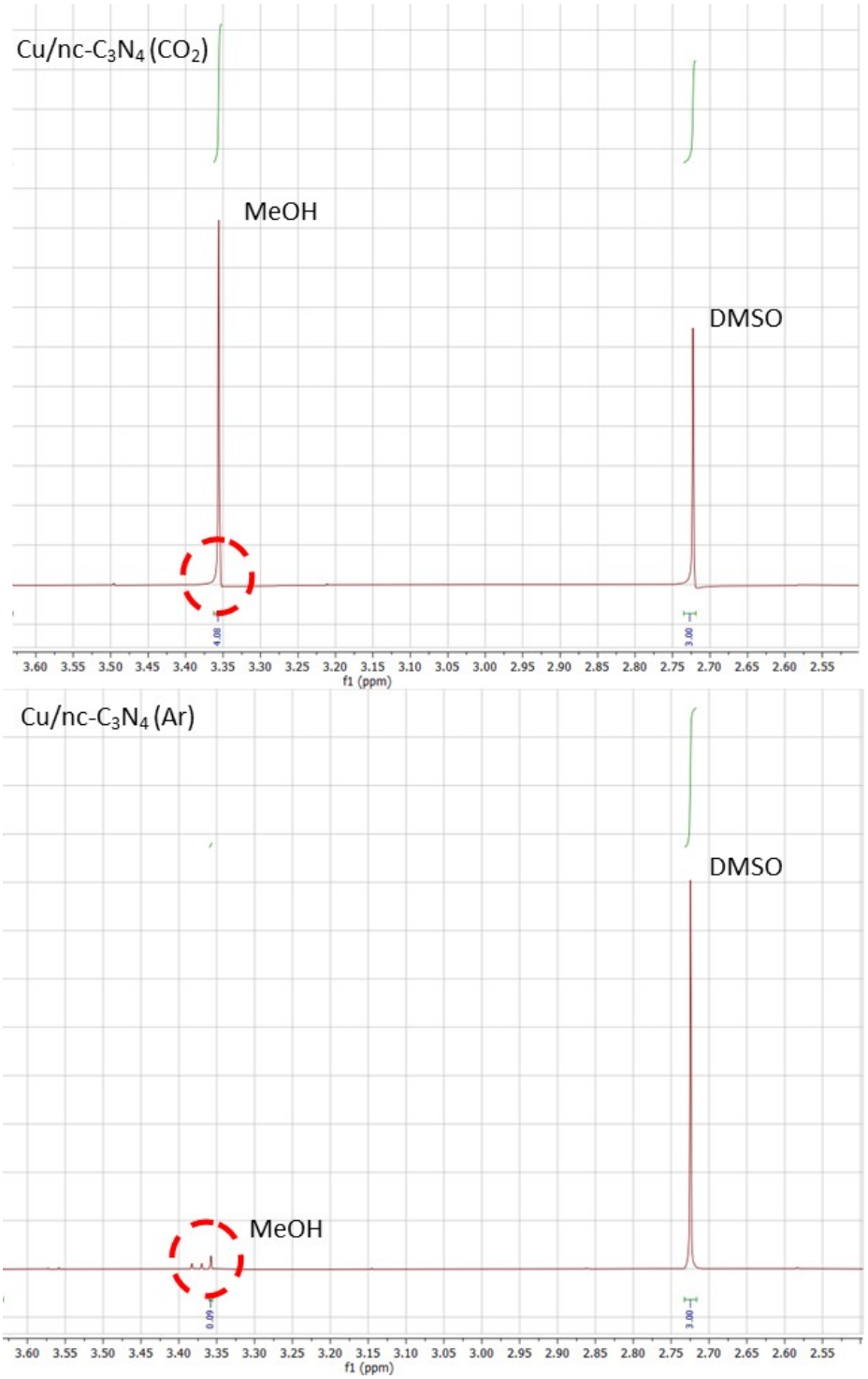

Figure S17. ^{1}H NMR spectroscopy analysis of methanol formed during CO_2 photoreduction across Cu/nc-C_3N_4 and a control reaction under Ar across Cu/nc-C_3N_4 which evidences the carbon source for methanol formation is CO_2.

References

1. A. Sasmal*, et al.*, *Chemical Communications*, 2013, **49**, 7806-7808.